

Reverse rotations in the circularly driven motion of a rigid body

Fernando Parisio

*Departamento de Física, Universidade Federal de Pernambuco, 50670-901, Recife, Pernambuco, Brazil
and Instituto de Física, Universidade Federal de Alagoas, 57072-970, Maceió, Alagoas, Brazil*

(Received 29 May 2008; published 11 November 2008)

We study the dynamical response of a circularly driven rigid body, focusing on the description of intrinsic rotational behavior (reverse rotations). The model system we address is integrable but nontrivial, allowing for qualitative and quantitative analysis. A scale-free expression defining the separation between possible spinning regimes is obtained.

DOI: [10.1103/PhysRevE.78.055601](https://doi.org/10.1103/PhysRevE.78.055601)

PACS number(s): 45.20.dc, 45.40.-f, 02.30.Ik

Nontrivial effects may arise in the realm of integrable classical mechanics. The most recent manifestation of this fact is the refreshed interest in the dynamics of sliding bodies [1]. In particular, the work by Farkas *et al.* [2], an investigation on the frictional coupling between translational and rotational motions, has deserved attention, being followed by a dozen of papers on related topics [3]. Most of these previous works address the influence of friction in the free (not driven) dynamics of disks. In the present paper we deal, in a sense, with a complementary problem, namely, that of the frictionless dynamics of a forced rigid body (RB). More specifically, we study the dynamical response of RB's subjected to rotational driving forces (in a way that will become clear below), focusing on the appearance of *reverse rotations*. Generally speaking, a reverse rotation occurs when a system, or part of it, is forced to rotate counterclockwise and its intrinsic angular degree of freedom develops a clockwise motion, or vice versa. This terminology has been recently used in the literature to designate unexpected rotational behavior of a cylinder inside a rotating drum filled with a viscous fluid [4]. Related though more intricate phenomena have been reported in the chaotic response of a parametrically excited pendulum [5], and in tests of printing machinery of journals [6]. Therefore, reverse rotations are quite a general behavior in diverse physical systems. In what follows we propose a simple mechanical model to investigate this effect in an analytical way.

Our model system is schematically shown in Fig. 1(a). It consists of a uniform disk of mass m and radius R resting on a horizontal frictionless surface. We consider a disk only for convenience, the following reasoning is valid for an arbitrary RB (this point will be discussed at the end of the paper). The system is then submitted to an external horizontal force \mathbf{F} , provided by a driving apparatus, through a thin rod attached to a fixed point (P) on the disk, around which the whole body can rotate freely. The driving apparatus takes the disk from rest and makes the point P follow a uniform circular trajectory of radius d around a fixed origin (O) with angular frequency ω [see Fig. 1(b)]. For definiteness we assume the rotation to be counterclockwise, and without loss of generality we use a coordinate system such that the point P lies in the positive x axis at $t=0$. For later times we denote the position vector of P by \mathbf{d} and the vector locating the center of mass (c.m.) by \mathbf{r} . Since the disk is assumed to be perfectly rigid, P is always a distance l apart from the c.m. The relative position of these two points is given by the vector \mathbf{l} , as

shown in Fig. 1(b). Finally, the angle between the x axis and the line connecting the c.m. and P is denoted by ϕ . The variables \mathbf{r} and ϕ completely specify the position of the disk.

The main goal of this work is to answer the following question: Which range of initial angles ϕ_0 and parameters m , ω , R , l , and d , lead to a clockwise rotation of the disk around P , if this is possible at all? The well-posedness of this question will become evident soon. Since the point P itself is being forced in the counterclockwise direction, such a dynamical response characterizes a reverse rotation [decreasing $\phi(t)$ on average].

According to our definitions, we have $\mathbf{d}=d\cos(\omega t)\hat{\mathbf{x}}+d\sin(\omega t)\hat{\mathbf{y}}$, where d can take any fixed value in the interval $(0, \infty)$. The vector \mathbf{l} linking the c.m. to P is given by $\mathbf{l}=l\cos\phi\hat{\mathbf{x}}+l\sin\phi\hat{\mathbf{y}}$, with $0<l\leq R$. The position of the c.m. is denoted by $\mathbf{r}=x\hat{\mathbf{x}}+y\hat{\mathbf{y}}$. These three vectors must satisfy $\mathbf{r}+\mathbf{l}=\mathbf{d}$, which provides two holonomic constraints: $x=d\cos(\omega t)-l\cos\phi$, and $y=d\sin(\omega t)-l\sin\phi$.

One can initially cope with the problem without being concerned with the question of how the disk came from rest to motion. This point will be addressed later. Suppose that \mathbf{F}_c , unknown *a priori*, is the constraint force that keeps the circular trajectory of P . This force is assumed to be provided by a robust apparatus in the sense that the circular path is not affected by the inertia of the disk. The equations of motion

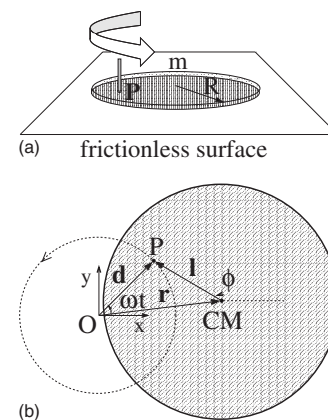


FIG. 1. (a) Circularly driven motion of a disk on a frictionless horizontal surface. (b) The point P , located by the vector \mathbf{d} , describes a circular path around the origin O . The vector \mathbf{r} gives the position of the center of mass (c.m.) and \mathbf{l} is the vector that connects the c.m. to P .

for the c.m. degrees of freedom read $F_{c,x}=m\ddot{x}$, $F_{c,y}=m\ddot{y}$. Newton's second law for the angular coordinate is given by $\boldsymbol{\tau}_c = \mathbf{l} \times \mathbf{F}_c = I_{c.m.} \ddot{\phi} \hat{\mathbf{z}}$, i.e.,

$$ml(\cos \phi \ddot{y} - \sin \phi \ddot{x}) = I_{c.m.} \ddot{\phi}, \quad (1)$$

where $I_{c.m.}$ is the inertia moment of the disk with respect to the center of mass [7]. By using the holonomic constraints we find $\ddot{x} = l \sin \phi \ddot{\phi} + l \cos \phi \dot{\phi}^2 - d\omega^2 \cos(\omega t)$ and $\ddot{y} = -l \cos \phi \ddot{\phi} + l \sin \phi \dot{\phi}^2 - d\omega^2 \sin(\omega t)$, one can, therefore, decouple the angular equation of motion, which becomes $ml\{d\omega^2[\sin \phi \cos(\omega t) - \cos \phi \sin(\omega t)] - l\ddot{\phi}\} = I_{c.m.} \ddot{\phi}$, or

$$\ddot{\phi} - \frac{mld\omega^2}{I_p} \sin(\phi - \omega t) = 0, \quad (2)$$

where $I_p = I_{c.m.} + ml^2$. As expected, the uniform plane rotation generates an effective gravity. We now proceed to the following change of variables: $\theta = \phi - \omega t + \pi$, implying $\dot{\theta} = \dot{\phi} - \omega$ and $\ddot{\theta} = \ddot{\phi}$. This change transforms Eq. (2) into the simple pendulum equation $\ddot{\theta} + (mld/I_p)\omega^2 \sin \theta = 0$. Thus, we see that the time dependence of ϕ , the physically relevant variable, is given by a combination of pendular and uniform motions (plus a constant additional factor),

$$\phi(t) = \theta_{\text{pendulum}}(t) + \omega t - \pi. \quad (3)$$

Note that solution (3) automatically yields $x(t)$, $y(t)$, and $\mathbf{F}_c(t)$. It also implies that we have a hidden constant of the motion corresponding to the mechanical energy of the auxiliary pendulum [we shall use this terminology to refer to the pendular term in the solution (3)] $\mathcal{E} = \frac{1}{2}I_p\dot{\theta}^2 + 2mld\omega^2 \sin^2(\theta/2)$, where the potential energy is set to zero in its lower position. In terms of initial conditions of the original variable we have

$$\mathcal{E} = \frac{1}{2}I_p(\dot{\phi}_0 - \omega)^2 + 2mld\omega^2 \cos^2(\phi_0/2). \quad (4)$$

By inspecting solution (3) we note that reverse rotations of the disk are possible only when θ_{pendulum} describes a motion of rotation instead of libration, that is, the mechanical energy of the auxiliary pendulum must satisfy $\mathcal{E} > 2mld\omega^2$ in negative pendular cycles. The relation (4) together with the equality $\mathcal{E} = 2mld\omega^2$ define the curves that separate libration and rotation of the variable θ in the space of initial conditions $(\phi_0, \dot{\phi}_0)$. One finds that initial conditions between the curves

$$\dot{\phi}_0 = \omega \left(1 \pm 2 \sqrt{\frac{mld}{I_p}} \sin(\phi_0/2) \right)$$

lead to libration of θ , and thus, to normal rotation of the disk. Of course, not all points that lie outside this region lead to the reverse behavior. The pendular rotation must be clockwise with an angular frequency larger than ω , in order to make $\phi(t)$ a decreasing function of t , on average. The condition for reverse rotation then reads $T = \sqrt{8I_p/\mathcal{E}K(\omega\sqrt{2mld/\mathcal{E}})} < 2\pi/\omega$, for clockwise pendular cycles of period T , where K denotes the complete elliptic function of first kind. In the regions where T equals $2\pi/\omega$, the constant \mathcal{E} satisfies the transcendental equation

$$K\left(\omega \sqrt{\frac{2mld}{\mathcal{E}}}\right) = \frac{\pi}{\omega} \sqrt{\frac{\mathcal{E}}{2I_p}}. \quad (5)$$

Using this prescription and Eq. (4) we manage to select the initial conditions $(\phi_0, \dot{\phi}_0)$ that lead to reverse and normal rotations. These regimes are separated by the curve

$$\dot{\phi}_0 = \omega - \sqrt{\frac{2\tilde{\mathcal{E}}}{I_p} - \frac{4mld\omega^2}{I_p} \cos^2(\phi_0/2)}, \quad (6)$$

where $\tilde{\mathcal{E}}$ stands for the solution of Eq. (5). The root with a plus sign was discarded because it is related to positive pendular rotations. We name the above-defined curve a synchronization line because initial conditions on it develop neither normal nor reverse rotation, for the angular frequency of θ coincides with ω and, therefore, the time evolution of ϕ averages to a constant value.

At this point we address the problem of static initial conditions. This is the most interesting situation, since it is expected that high enough clockwise initial velocities $\dot{\phi}_0$ trivially lead to reverse rotations. We note, however, that \dot{x} , \dot{y} , and $\dot{\phi}$ never vanish simultaneously, and, thus, the kinetic energy of the disk $\mathcal{K} = m\dot{x}^2/2 + m\dot{y}^2/2 + I_{c.m.}\dot{\phi}^2/2 = md^2\omega^2/2 + (I_p\omega/2 + mld\omega - \mathcal{E}/\omega)\dot{\phi} - I_p\dot{\phi}^2/2 + I_p\dot{\phi}^3/2\omega$, is nonzero for all times. It is clear that the force \mathbf{F}_c alone is not compatible with static initial conditions. In order to encompass these conditions, we assume that an impulsive force acts on the disk, taking it from rest to motion in a time scale much shorter than any other in the problem, e.g., $2\pi/\omega$. This is a realistic assumption when we have a table top engine driving a light body. More explicitly, we suppose that the force can be split into two parts,

$$\mathbf{F} = \begin{cases} \mathbf{F}_0 & \text{for } t \in [0^-, 0^+], \\ \mathbf{F}_c & \text{for } t > 0^+, \end{cases} \quad (7)$$

where \mathbf{F}_0 denotes the impulsive force that acts during an arbitrarily small time interval centered at $t=0$. In the limiting case we have a δ function, which we initially write in generic form as $\mathbf{F}_0 = \delta(t)(\alpha\hat{\mathbf{x}} + \beta\hat{\mathbf{y}})$, where α and β have dimension of momentum. These constants are to be determined by the motion we know the force \mathbf{F}_0 causes to the disk. More specifically, we know that, immediately after its application, to fit the \mathbf{F}_c prescription, the point P must acquire a velocity

$$\mathbf{v}_P(0^+) = \omega d \hat{\mathbf{y}}. \quad (8)$$

The equations of motion in the infinitesimal interval $[0^-, 0^+]$ are $m\ddot{x} = \alpha\delta(t)$, $m\ddot{y} = \beta\delta(t)$, and $l \cos \phi \beta\delta(t) - l \sin \phi \alpha\delta(t) = I_{c.m.} \ddot{\phi}$. Integrating, one obtains the velocities soon after the application of \mathbf{F}_0

$$\dot{x}(0^+) = \frac{\alpha}{m}, \quad \dot{y}(0^+) = \frac{\beta}{m}, \quad \dot{\phi}(0^+) = \frac{l}{I_{c.m.}}(\beta \cos \phi_0 - \alpha \sin \phi_0), \quad (9)$$

where, here, the static initial conditions were employed: $\dot{x}(0^-) = 0$, $\dot{y}(0^-) = 0$, and $\dot{\phi}(0^-) = 0$. We also used $\phi(0^-) = \phi(0^+) = \phi_0$ (since the impulsive force causes no discontinuity).

ity in coordinates). The velocity of P at any time is given by $\mathbf{v}_P = \dot{\mathbf{r}} + \dot{\mathbf{l}} = (\dot{x} - l\dot{\phi} \sin \phi)\hat{\mathbf{x}} + (\dot{y} + l\dot{\phi} \cos \phi)\hat{\mathbf{y}}$. Therefore, the initial velocity as a function of α and β is

$$\mathbf{v}_P(0^+) = \left(\frac{\alpha}{m} - \frac{l^2}{I_{c.m.}} \sin \phi_0 (\beta \cos \phi_0 - \alpha \sin \phi_0) \right) \hat{\mathbf{x}} + \left(\frac{\beta}{m} + \frac{l^2}{I_{c.m.}} \cos \phi_0 (\beta \cos \phi_0 - \alpha \sin \phi_0) \right) \hat{\mathbf{y}}.$$

By applying the consistency condition (8) we obtain a pair of equations, involving α and β , whose solution is

$$\alpha = \frac{\omega d m^2 l^2}{I_P} \sin \phi_0 \cos \phi_0, \quad \beta = m d \omega \left(1 - \frac{m l^2}{I_P} \cos^2 \phi_0 \right).$$

We then found the impulsive force that is consistent with the subsequent evolution of the system. Substituting the above results in the last equation in (9), we obtain a quite simple relation between the initial angle ϕ_0 and the initial velocity $\dot{\phi}_0$ (where we suppress the argument 0^+). Given the initial angle of the static disk, the angular velocity it acquires immediately after the driving apparatus is turned on is

$$\dot{\phi}_0 = \frac{m d l \omega}{I_P} \cos \phi_0. \quad (10)$$

Only pairs $(\phi_0, \dot{\phi}_0)$ related through this expression are valid initial conditions. We are now in position to show the relevant regions and curves in the space of initial conditions. In Fig. 2(a) we show the normal (blank) and reverse (dotted) regions in the space $(\phi_0, \dot{\phi}_0)$, separated by the synchronization line (gray curve). The black line represents the possible initial conditions as given by (10). We used the following parameters: $\omega = 6$ rad/s ($\nu \sim 1$ Hz), $m = 100$ g, $R = 10$ cm, $l = 7$ cm, and $d = 10$ cm. For these values, the constant of the motion that satisfies Eq. (5) is $\tilde{\mathcal{E}} \approx 0.0543$ J. We see that, for these parameters, no reverse rotations can occur (the black curve does not reach the dotted region). In contrast, if we set $d = 40$ cm, keeping the other parameters (leading to $\tilde{\mathcal{E}} \approx 0.2017$ J), we obtain the result displayed in Fig. 2(b), where it is clear (the gray and black curves cross each other) that reverse rotations take place for an interval of initial angles centered at $\phi_0 = \pi$. The three initial conditions marked with a square, a circle, and a triangle represent the possible regimes normal rotation, synchronization, and reverse rotation. The time evolution of ϕ for these three conditions is shown in Fig. 3. The corresponding initial angles in radians are $\phi_0 \approx 2.20$ (black), $\phi_0 \approx 2.44$ (gray), and $\phi_0 \approx 2.68$ (light gray). Notice that in the black curve, e.g., we have normal and reverse instantaneous motions depending on the instant at which we record the velocity $\dot{\phi}$. The results presented in Fig. 2 refer to the global behavior of ϕ .

It is possible to establish in a more precise way which initial configurations lead to reverse rotations. First we note that the range of initial angles that lead to reverse behavior is bounded by the intersections of the synchronization line (6) and the initial condition curve (10). These boundary angles are given by

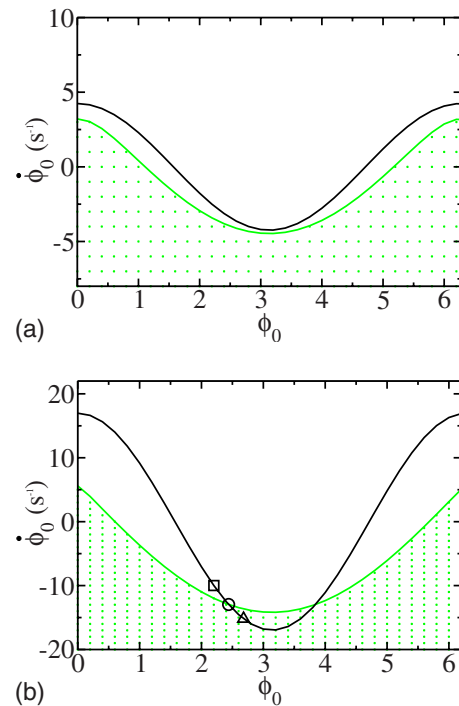


FIG. 2. (Color online) Dotted regions represent initial conditions leading to reverse rotations. We set $d = 10$ cm in (a) and $d = 40$ cm in (b). The gray and black lines are the synchronization and initial condition curves, respectively. In (a) no reverse rotations can develop since the two lines do not cross. In (b) reverse behavior is possible for an interval centered at $\phi_0 = \pi$.

$$\cos^2 \phi_0^{(b)} = \frac{I_P^2}{(m d l \omega)^2} \left(\frac{2\tilde{\mathcal{E}}}{I_P} - \frac{2m d l \omega^2}{I_P} - \omega^2 \right). \quad (11)$$

Since $0 \leq \cos^2 \phi_0^{(b)} \leq 1$, in order to get reverse rotations we must have

$$2m d l + I_P < \frac{2\tilde{\mathcal{E}}}{\omega^2} < \frac{1}{I_P} (I_P + m d l)^2, \quad (12)$$

where we have a condition imposed on $\tilde{\mathcal{E}} = \tilde{\mathcal{E}}(m, d, l, I_P, \omega)$. Let us analyze the limiting cases $2\tilde{\mathcal{E}}/\omega^2 = 2m d l + I_P$ and $2\tilde{\mathcal{E}}/\omega^2 = (1/I_P)(I_P + m d l)^2$. Substituting these expressions in the transcendental equation (5), we obtain relations invol-

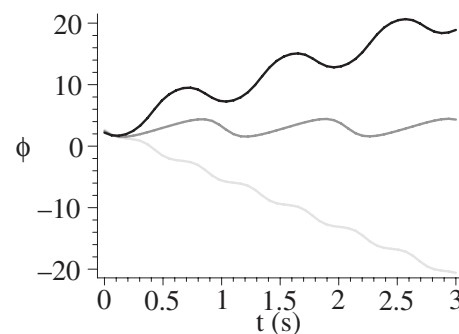


FIG. 3. Evolution of the initial conditions indicated in Fig. 2(b): square (black), circle (gray), and triangle (light gray).

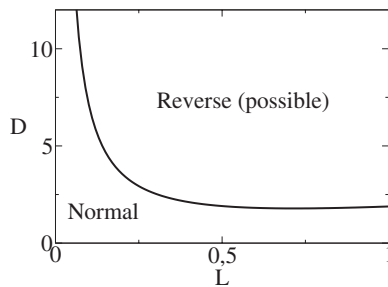


FIG. 4. Configurations located above the curve may develop reverse rotations. Below the curve only normal rotation is possible.

ving a *single* parameter, $K[\sqrt{2\sigma/(\sigma+1)}]=(\pi/2)\sqrt{\sigma+1}$ and $K[2\sqrt{2\sigma/(\sigma+2)}]=(\pi/4)(\sigma+2)$, respectively, with $\sigma=2mdl/I_p$. The first equation has only the solution $\sigma=0$, which is physically trivial, implying that the left-hand side of the inequality (12) is always satisfied. The second equation, besides $\sigma=0$, presents the solution $\tilde{\sigma}\approx 2.523$. Thus initial configurations obeying $2mdl/I_p=\tilde{\sigma}$ separate regions where reverse rotation is possible from regions where only normal rotations can occur. This condition involves only the relative scales $D=d/R\in(0,\infty)$ and $L=l/R\in(0,1)$ and, in the case of a disk, reads

$$D=0.631L^{-1}+1.261L. \quad (13)$$

The above result is universal, in the sense that it is valid for any m and ω , and is independent of the absolute scales R , l , and d . As indicated in Fig. 4, initial geometrical configurations located below the curve (13) always lead to normal behavior, while configurations above it may enable reverse rotations, depending on the initial angle ϕ_0 [the precise values of ϕ_0 are given by Eq. (11)]. We also note that there is a value of d below which no reverse rotation occur. It is given by $D_{\min}=\tilde{\sigma}/\sqrt{2}$, that is, $d_{\min}=1.784R$. For $L>0.5$, variations in this parameter produce virtually no change in D , which becomes the only relevant parameter to define the possible regimes of the system (see the “plateau” in Fig. 4).

We stress that the obtained results are very general since we used the particular form of I_p only to obtain Eq. (13). For

an arbitrary RB we have $I_p=ml^2+\gamma m\mathcal{R}^2$, where γ is a number and \mathcal{R} is a characteristic scale. For the disk we have $\gamma=1/2$ and $\mathcal{R}=R$, while for a rectangular plate of sides a and b we have $\gamma=1/12$ and $\mathcal{R}=\sqrt{a^2+b^2}$. The general form of Eq. (13) is

$$D=\frac{\tilde{\sigma}}{2}(\gamma L^{-1}+L), \quad (14)$$

with $D=d/\mathcal{R}$ and $L=l/\mathcal{R}$, for $\mathcal{R}\neq 0$. We note that in the “degenerate” case of a point mass connected by a massless rod to the pivotal point, obtained from the disk by taking $R=0$, we get $\sigma=2d/l$ and the reverse condition becomes a one-parameter relation $d/l>1.261$.

We investigated reverse rotations in the circularly driven motion of a RB whose intrinsic angular degree of freedom was shown to evolve according to a combination of pendular and uniform motions. This enabled the complete determination of the initial configurations that lead to reverse behavior [Eq. (12)]. In addition, a scale-free, purely geometrical relation defining the regions where reverse rotation is possible was obtained [Eq. (14)]. The effects of friction, assumed to be negligible in this work, may play an interesting role. The friction generated in the small contact area connecting the thin rod and the RB gives an extra torque (but no net force). This may be the only friction in the problem if we assume that the RB is kept in the horizontal position solely by the rod. It may also be of interest to consider the system immersed in a viscous fluid. This would make our apparatus very similar to a bioreactor for tissue growth [8]. It seems that the influence of the regime of intrinsic rotation of the tissue construct (our disk) is yet to be analyzed. These pending issues are presently under investigation.

The author thanks G. L. Vasconcelos, M. A. F. Gomes, and P. H. Figueiredo for helpful discussions. J. A. Miranda is acknowledged for a critical reading of the manuscript. This work was partially supported by the Brazilian agencies CNPq and FACEPE (Grants No. DCR 0029-1.05/06 and No. APQ 0800-1.05/06).

- [1] T. C. Halsey, *Nature (London)* **424**, 1005 (2003).
 [2] Z. Farkas, G. Bartels, T. Unger, and D. E. Wolf, *Phys. Rev. Lett.* **90**, 248302 (2003).
 [3] See, for example, D. E. Wolf, S. R. Dahmen, and H. Hinrichsen, *Int. J. Mod. Phys. B* **21**, 4158 (2007); P. D. Weidman and C. P. Malhotra, *Physica D* **233**, 1 (2007); *Phys. Rev. Lett.* **95**, 264303 (2005); S. R. Dahmen, Z. Frakas, H. Hinrichsen, and D. E. Wolf, *Phys. Rev. E* **71**, 066602 (2005); S. R. Dahmen, H. Hirichsen, A. Lysov, and D. E. Wolf, *J. Stat. Mech.: Theory Exp.* (2005) P033004; M. Dutt and R. P. Behringer, *Phys. Rev. E* **70**, 061304 (2004); M. Einax, M. Schulz, and S. Trimper, *ibid.* **70**, 046113 (2004); E. T. Jensen and M. R. A. Shegelski,

- Can. J. Phys.* **82**, 791 (2004).
 [4] J. R. T. Seddon and T. Mullin, *Phys. Fluids* **18**, 041703 (2006).
 [5] K. Yoshida and K. Sato, *Int. J. Non-Linear Mech.* **33**, 819 (1998).
 [6] S. DeCamillo, K. Brockwell, and W. Dmochowski, *Tribol. Trans.* **49**, 305 (2006).
 [7] We recall that any referential attached to the disk is noninertial. The validity of Eq. (1) can be checked by writing the angular equation of motion in the inertial referential: $\mathbf{d}\times\mathbf{F}_c=d\mathbf{L}/dt$, where $\mathbf{L}=m\mathbf{r}\times\dot{\mathbf{r}}+I_{c.m.}\dot{\phi}\hat{\mathbf{z}}$, and using the relation $\mathbf{r}+l=\mathbf{d}$.
 [8] L. J. Cummings and S. L. Waters, *IMA J. Math. Med. Biol.* **24**, 169 (2007).